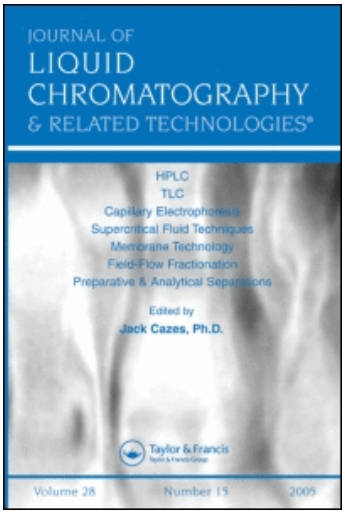

Journal of Liquid Chromatography & Related Technologies
Publication details, including instructions for authors and subscription information:
http://www.informaworld.com/smpp/title~content=t713597273

Flow Fluctuations in GPC-Viscometry

J. Lesec[a]
[a] CNRS URA#278 - ESPCI, Paris, Cedex, France

To cite this Article Lesec, J.(1994) 'Flow Fluctuations in GPC-Viscometry', Journal of Liquid Chromatography & Related Technologies, 17: 5, 1011 — 1028
To link to this Article: DOI: 10.1080/10826079408013383
URL: http://dx.doi.org/10.1080/10826079408013383

JOURNAL OF LIQUID CHROMATOGRAPHY, 17(5), 1011-1028 (1994)

FLOW FLUCTUATIONS IN GPC-VISCOMETRY*

JAMES LESEC
CNRS URA#278 - ESPCI
10 rue vauquelin
75231 - Paris cedex 05 - France

INTRODUCTION

GPC-Viscometry requires a molecular weight calibration curve, usually a "Universal calibration curve" (1) Log ([η]*M) = f (Ve). With classical GPC, using only one concentration detector, perfect control of solvent flow rate is required since molecular weights of broad polymers are calculated by comparison of their sliced distributions with elution volumes of narrow standards. Data acquisition being performed as a function of time, this comparison can be achieved accurately only when both experiments are run at exactly the same flow rate. A small error in flow rate introduces a significant error in molecular weight because of the logarithmic scale of the calibration curve.

The purpose of this paper is not to discuss this kind of problem, but to study the consequence of very small flow fluctuations. These fluctuations are unable to introduce a significant error in molecular weights when referring to a calibration curve, but they lead to very small peak distortions with flow-sensitive detectors like the Single Capillary Viscometer (SCV) (2-6) and, consequently, to errors in data interpretation.

THE SINGLE CAPILLARY VISCOMETER.

The Single Capillary Viscometer (SCV) used in the WATERS GPC 150CV instrument (7) is described in Figure 1. It is composed of a capillary tube

* paper presented at the WATERS Int'l GPC symposium, SAN FRANCISCO, october 1991.

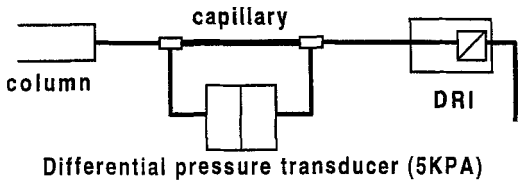

Capillary characteristics
Diameter = 15/1000"
Length = 6" (15 cm)
Internal volume = 18 µl

Performance in THF at 1 ml/mn and 35°C
Shear rate = 2800 s^{-1}
Reynolds = 120
Differential pressure = 2 KPA (20 mbars)
Working pressure = 200 KPA (2 bars)

Figure 1. The Single Capillary Viscometer (SCV).

with the following characteristics (length=6", internal diameter=0.014") and of a differential pressure transducer connected to both capillary ends to measure the pressure drop across the capillary.

SCV obeys Poiseuille's law and the pressure drop P across the capillary depends on the capillary geometry (radius r and length l), on the flow rate Q and on the viscosity of fluid η according to:

$$P = 8 / \pi * l / r^4 * \eta * Q$$

At constant flow rate Q, the pressure drop is proportional to viscosity η and at constant viscosity η, the pressure drop is proportional to flow rate Q. Consequently, in order to use the SCV as an accurate viscometer, the flow rate must be maintained absolutely constant during the GPC experiment. Conversely, SCV allows perfect control of flow rate and can also be used as a very powerful troubleshooting tool.

The purpose of this paper is to demonstrate that, when using a SCV for viscometry measurements and assuming a very constant flow that is not strictly observed, the viscometer function may be corrupted by a very small flow fluctuation, leading to erroneous interpretation of viscometry data.

EVIDENCE OF A FLOW FLUCTUATION.

Origin of the flow fluctuation.

Figure 2 represents the block diagram of the GPC/Viscometry experiment. For our purpose, the important part of the design is the detector area where restrictions occur because of the presence of capillary tubes (0.009"). These low diameter tubings are usually used as connecting tubes but also as detector inlet tubings (Differential Refractive Index detector - DRI) in order to minimize dead volumes.

In GPC, the problem is we are using high molecular weight samples that increase the viscosity of solvent. As the viscosity of pure solvent is η_0, when a polymer is dissolved it becomes η using the following relationship in a first approximation:

$$\eta = \eta_0 * (1 + [\eta] * C)$$

C is the sample concentration and $[\eta]$ the sample intrinsic viscosity that varies with molecular weight M according to:

$$[\eta] = K * M^{a}$$

K and **a** being the Mark-Houwink coefficients ($0.5 > \mathbf{a} > 0.8$ for coil polymers).

The parameter $[\eta]*C$ represents the increase of solvent viscosity due to the presence of polymer. Consequently, when the polymer solution enters the detector area, the viscosity of fluid increases, and, according to the Poiseuille's law above-described, the pressure drop in detectors increases proportionally, leading to an increase of the total back pressure in the system. This increase is very weak, since polymers are very diluted, but depends on the parameter $[\eta]*C$; nevertheless this is the origin of the flow fluctuation.

The flow fluctuation.

When the polymer comes across the columns, the system is in pressure equilibrium. When the polymer comes across the detectors, the previous equilibrium is disturbed according to two phases:

- phase #1 - When the polymer enters into the detectors, there is an increase of pressure leading to a momentary decrease of flow rate to reach another equilibrium. The pumping system being at constant flow rate, the system

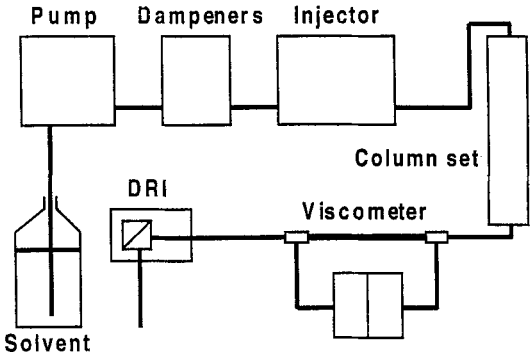

Figure 2. Block diagram of the GPC/Viscometry experiment.

(dampeners and columns) accumulates some solvent and gives a negative wave in flow rate at the outlet.

- phase #2 - When the polymer elutes from the detectors, there is a decrease of pressure leading to a momentary increase of flow rate. The system (dampeners and columns) which has previously accumulated some solvent, releases the solvent and now gives a positive wave in flow rate at the outlet to reach another equilibrium.

In fact, the detector volume being very small with regard to the peak volume, the two phenomena (phase #1 and phase #2) occur quite simultaneously. Consequently, it is impossible to obtain the two waves separately but only their resultant overlay, since they occur at different times that correspond only to the detector volumes. This is represented in Figure 3.

The consequence of this flow fluctuation on the viscometer profile is represented in figure 4. The real peak and the flow fluctuation are overlaid in 4a. The composition of the two signals is represented in 4b where the dashed line corresponds to the real peak and the solid line to the experimental peak. Obviously, a peak distortion occurs which leads to an experimental peak that looks to be moved downstream. It is a peak distortion but it looks like a peak shift, this is why this effect conflicts with interdetector volume correction, as we shall see later. It should be noted here that a very small fluctuation is enough to produce a significant apparent peak shift.

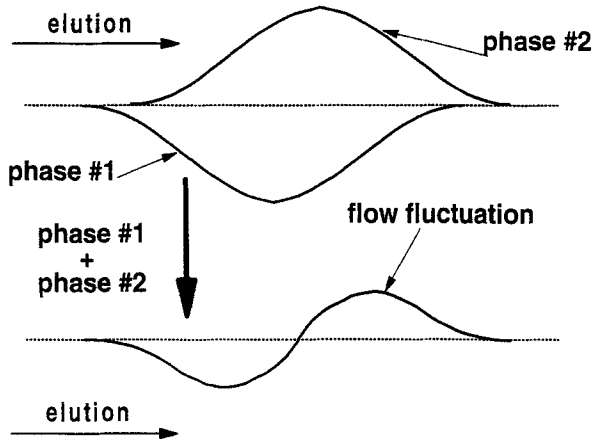

Figure 3. The flow fluctuation, summation of two fluctuations.

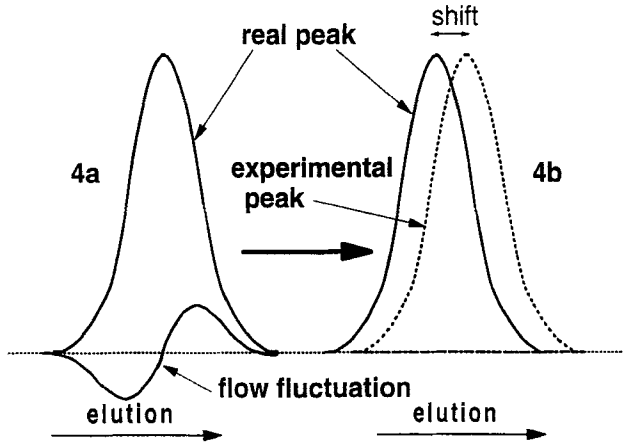

Figure 4. Viscometer profile distortion by a flow fluctuation.

Computer simulation.

A computer simulation was performed in order to verify the hypothesis of the flow fluctuation. The chromatographic system is represented as slices of solvent, each slice having a volume of 20 µl. The following conditions were used:

- the column set is represented by a long tubing with an internal diameter of 0.017" based on the equivalence of a volume of 11 ml and a pressure drop of 6 bars which is the normal behavior of a column set at 1 ml/mn of THF. (high number of 20 µl slices).

- the viscometer is represented by a tubing with 0.014" I.D. and one 20 µl slice (which is very close to the reality 18 µl).

- the refractometer inlet capillary is represented by a tubing with 0.009" I.D. and five 20 µl slices (which represents approximately its common internal volume, 80-100 µl).

- the refractometer outlet tube is represented by a tubing with 0.040" I.D. with a large number of 20 µl slices (the pressure drop in this tubing is negligible anyway).

In the simulation, these four volumes are connected in series and in this sequence. A gaussian viscosity profile is entered into the simulation to simulate the detection of a viscometer peak. The total pressure drop is then computerized for pure THF using the Poiseuille's relationship by the summation of individual pressure drops of each slice. From the viscosity profile, three different parameters can be calculated: the pressure profile, the flow profile and the distorted viscosity profile. They are represented in Figure 5.

- the pressure profile - The excess of pressure starts at a non-zero value because of the previous presence of the polymer in the columns. Then it increases when the polymer enters into the DRI inlet tubing then decreases when it enters the outlet tubing. We can observe that the final pressure value is smaller than the starting pressure value, since the system was first at equilibrium with the polymer in a 0.017" tubing and at the end it is in a 0.040" tube (which is roughly zero excess of pressure).

- the flow profile - It is represented in arbitrary units and starts at a value of 4, which corresponds to the nominal value of flow rate (the system being at equilibrium). It decreases to a value of 2 when the polymer enters into the DRI inlet tubing, then it increases to approximately a value of 6.6 and returns to the

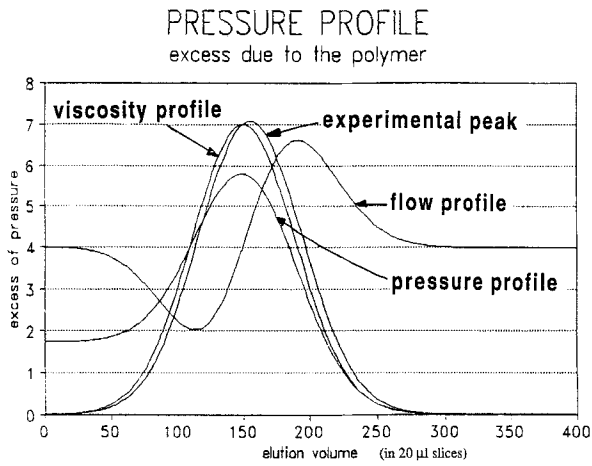

Figure 5. Computer simulation of the flow fluctuation and the viscometric signal distortion on a standard instrument.

previous equilibrium value of 4 (nominal flow rate). THIS IS THE TYPICAL FLOW FLUCTUATION. We can observe that this fluctuation is not symmetrical, due to the fact that the pressure fluctuation profile is not symmetrical either. This reason has been previously explained.

- the distorted viscosity profile (experimental peak) - It is calculated by adding the viscosity profile to the flow fluctuation profile using an attenuation coefficient to take into account the difference in scale (the flow profile being expanded to become visible since it is a weak effect). We can see in Figure 5 that the distortion of the viscosity profile looks like a small shift towards high elution volumes as previously predicted.

Experimental evidence.

In order to evidence this phenomenon experimentally and, as it was impossible to eliminate this effect in a first step, two sets of experiments were performed with two different settings represented in Figure 6.

- instrument #1 is the standard Waters model 150CV.

- instrument #2 is the same instrument with a restrictor (long 0.009" I.D. capillary tube) inserted between the column set and the detectors. This device does not

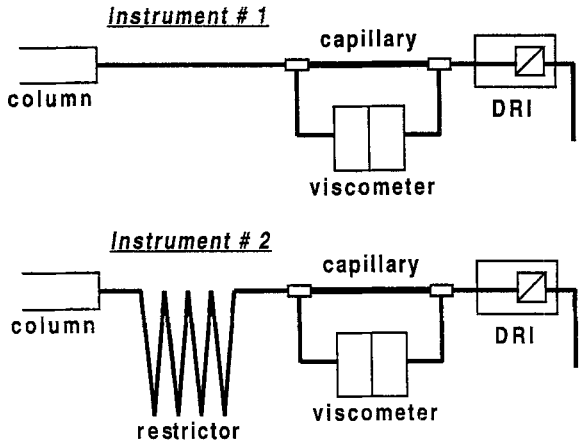

Figure 6. Schematics of instrument #1 and instrument #2.

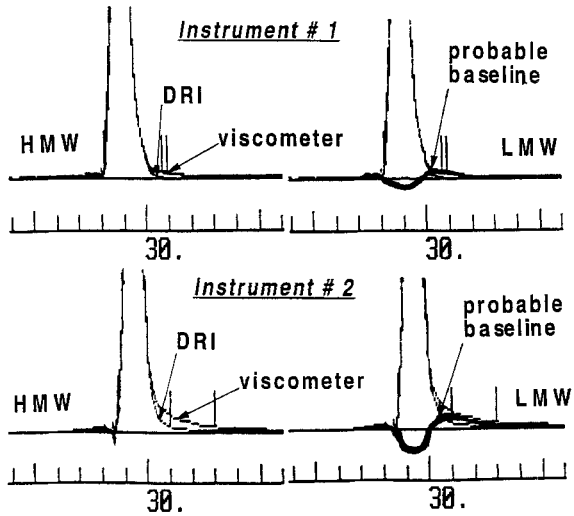

Figure 7. Influence of the flow fluctuation on the elution profile of the narrow polystyrene standard 355K.

change the interdetector volume at all and, with regard to the DRI peak, the viscometer peak has no reason to move. The advantage of this setting is not to correct the effect but to amplify it, since the presence of the restrictor should normally increase the pressure drop in the detector area and, consequently, the intensity of the pressure fluctuation.

The results are represented in Figure 7 where a narrow polystyrene standard 355K has been injected into both instruments under exactly the same conditions. On instrument #1, we can observe on peak feet (top, left) an abnormal behavior of the viscometer peak since, in the low molecular weight region, the viscometer response is a little bit stronger than the DRI one, which is impossible. The DRI response being as C and the viscometer response being as $C^*[\eta]$, the viscometer response should be smaller than the DRI response in the low molecular weight region. Also, we can suspect a flow fluctuation represented (top, right).

On instrument #2, the phenomenon is much more obvious. We can observe that the viscometer signal (bottom, left) is significantly above the DRI signal and, even at the beginning of the peak, there is a small sharp decrease of the signal that is very probably the beginning of the flow fluctuation. It is easy to imagine the probable baseline under the peak that is drawn in Figure 7 (bottom, right). So, increasing the pressure drop in the detector area increases the effect. That demonstrates that the pressure drop in detectors is really responsible for the flow fluctuation.

The interdetector volume correction.

The interdetector volume correction is indirectly involved here since the consequence of the flow fluctuation is an apparent peak shift. The two detectors are connected in series and the slice data acquisition is usually performed simultaneously on both detectors. In order to match the slice information coming from the two detectors, it is then necessary to correct the viscometer slice retention volumes to take into account the time necessary for one molecule to move from the viscometer to the DRI. This is what is called the "interdetector volume correction".

As the flow fluctuation abnormally moves the viscometer peak downstream, it is possible to use the interdetector volume correction to study the consequence of the flow fluctuation. As we shall see, using the correct value of interdetector volume leads to erroneous results, but using an underestimated value may lead to correct results, the flow fluctuation shift being corrected by this too-small interdetector volume correction.

Consequence on data interpretation.

The consequence of the flow fluctuation on data interpretation is exactly the same as a wrong interdetector volume correction. There is a mismatch between the slice concentration information C_i from the DRI and the slice pressure information $[\eta]_i*C_i$ from the viscometer. $[\eta]_i$ being calculated by dividing $[\eta]_i*C_i$ by C_i; the mismatch leads to a wrong calculation of $[\eta]_i$. As this effect is very weak, the errors on $[\eta]_i$ are almost negligible and the average $[\eta]$ is generally calculated well. BUT, AND THIS IS THE MAIN ISSUE, THE ERRORS ARE NOT SYMMETRICAL. When the viscometer peak is moved downstream for example, $[\eta]_i$ is calculated a little bit too small in the HMW region and a little bit too high in the LMW region, leading to a slight rotation of the Mark-Houwink plot and a slight decrease of the Mark-Houwink **a** exponent. THIS IS THE MAIN CONSEQUENCE OF THE FLOW FLUCTUATION.

Unfortunately, when running a GPC-Viscometry experiment, we are very concerned with the exponent **a** value that has a physical meaning (**a**=0.5 for poor solvents, **a**=0.8 for good solvents, higher value for rigid polymers). Also, for branched polymers, the branching distribution g'_i being calculated by dividing the experimental intrinsic viscosity $[\eta]_i$ by the $[\eta]_i$ value of the corresponding linear polymer at the same MW, the calculation of the branching distribution would be also affected by this effect. For these reasons, the flow fluctuation must be corrected if possible or eliminated by a modification of the hardware.

EXPERIMENTAL RESULTS.

The evidence of the flow fluctuation was firstly described in 1991 (8-9) using the analysis of several broad distribution polystyrene samples. Table 1 shows typical results obtained with the polystyrene DOW 1683 using a standard Model 150 CV having an interdetector volume (offset) of around 80 µl (geometrical value). The Mark-Houwink K and **a** coefficients were measured with 11 polystyrene narrow standards (**a**=0.71, logK=-1.8775).

This result shows that, when using the correct value of interdetector volume, a too small value is obtained for **a**, the correct value being obtained using

Table 1 - Mark-Houwink **a** determination on DOW 1683.

Offset used (in µl)	**a** exponent
80 (geometrical)	0.6
-20 (corrected)	0.71

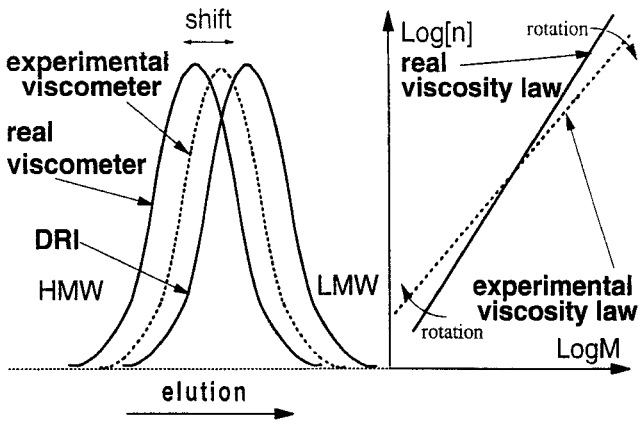

Figure 8. Viscometer peak shift and rotation of the Mark-Houwink law.

an interdetector volume correction of -20 µl. This means that the flow fluctuation has moved the viscometer peak downstream by 100 µl, which is a small effect but which is enough to make a decrease of the **a** Mark-Houwink exponent from 0.71 to 0.6.

It is important to notice that this 100 µl apparent shift, and consequently, the decrease of the **a** exponent from 0.71 to 0.6, is induced by a very weak flow fluctuation. Its maximum intensity has been estimated to be around 4% of the maximum deviation of the viscometer peak. In the DOW 1683 conditions, at a flow rate of 1 ml/mn, the maximum deviation of the viscometer signal corresponds to an equivalent flow variation of 0.01 ml/mn. 4% of this value leads to a maximum flow fluctuation value of 0.0004 ml/mn.

Nevertheless, this extremely weak variation in flow (0.4 µl/mn, that is 0.04%) significantly disturbs the viscometry calculation and leads to a decrease of the **a** exponent from 0.71 to 0.6.

Obviously, this kind of extremely weak fluctuation 0.04% cannot lead to any problems in the calculation of molecular weights when referring to the calibration curve; only the Mark-Houwink plot rotates a little bit. This effect demonstrates the very high general quality of the flow control in the Waters GPC 150CV instrument, based on the use of the Single Capillary Viscometer as a flow controller.

Other evidence is given in Table 2 where results on instrument #1 and instrument #2 (previously described) are compared.

Table 2 - Mark-Houwink **a** determination function of pressure drop.

Offset used (in µl)	**a** (instrument #1)	**a** (instrument #2)
80 (geometrical)	0.6	0.52
- 20 (corrected)	0.71	0.63

Table 3 - Measurements of peak elution volumes in ml.

Difference (DRI-Visco)	NBS 706	DOW 1683	Offset
Theoretical	0.847	1.224	0
Instrument #1	0.747	1.125	0.100
Instrument #2	0.691	1.079	0.150

Table 4 - Measurements of broad polystyrene samples.

Samples	Mw_{ps}	Mw_{univ}	[η]	**a**	LogK
DOW1683-labo	242,600	245,800	81.8	0.709	-1.873
DOW1683-elf	241,300	241,900	82.5	0.708	-1.866
NBS706-labo	261,300	257,000	90.7	0.715	-1.888
NBS706-elf	258,800	256,900	88.6	0.715	-1.895
BASF168N-labo	303,700	302,500	99.6	0.682	-1.712
BASF168N-elf	316,900	319,200	101	0.689	-1.760
PS-IUPAC	217,600	213,600	77.9	0.705	-1.831
PS1240-elf	305,600	300,000	101.5	0.707	-1.840

For instrument #1, we get the same result than in Table 1. For instrument #2, we observe a stronger effect leading to smaller a values. It has not been possible to correct the used offset to obtain the right value 0.71 for instrument #2, the software not allowing too negative offset values.

A further evidence is reported in Table 3 by the measurement of the differences in retention volumes at the peak apex between the viscometer and the DRI for DOW 1683 and NBS 706 on both instruments.

The measurements of peak retention volumes confirm a viscometer peak shift downstream depending upon pressure drop in the detector area: 100 µl for instrument #1 and 150 µl for instrument #2.

Nevertheless, it was possible to analyze several broad distribution polymers using the corrected value of interdetector volume of -20 µl. Instrument

used is a Waters 150 CV at a temperature of 40°C with THF as eluent at 1 ml/mn. The column set was composed of four Waters Ultrastyragel 10^3, 10^4, 10^5 and 10^6 Å. For each sample, 400 µl were injected at a concentration of 0.1%. Broad polystyrene samples were analyzed using a polystyrene calibration to check the behavior of universal calibration. Mw_{ps} are molecular weights in PS units (classical GPC) and Mw_{univ} are molecular weights in real units by GPC-Viscometry. They are listed in Table 4 with viscometry results. The viscosity law obtained using 11 narrow distribution standards was: **a**=0.710, LogK=-1.8775.

We observe a good correlation of molecular weights and viscosity parameters. Nevertheless, Table 4 contains original results of the very first experiments in March 1990. With regard to more recent results, the molecular weight values listed in Table 4 are too low by approximately 4% due to an imperfect calibration curve. The same holds true for intrinsic viscosity [η] values that are also too low by approximately 4%, but because the injector volume was not properly calibrated. The 150CV injector is a very reproducible injection system but needs to be carefully calibrated to know the exact amount of injected polymer, this one being used in viscosity calculations.

DISCUSSION.

Parameters influencing the flow fluctuation.

As we have seen, the flow fluctuation effect is induced by viscosity problems. It depends, accordingly, upon the specific viscosity of the polymer solution, that is [η]*C. This means that the effect depends upon both sample concentration and molecular weight (proportional to intrinsic viscosity [η]); the higher the parameter [η]*C, the stronger the fluctuation and the stronger the peak shift, as shown in Figure 9.

Conversely, the length of the perturbation will depend upon the length of the viscosity profile, that is roughly the sample polydispersity. The higher the polydispersity, the longer the flow fluctuation profile and the stronger the peak shift, as shown in Figure 10.

This can be observed by carefully looking at the a values in Table 4 where the offset value -20 µl was adjusted for the DOW 1683. Obviously, for this sample, the right **a** value is perfectly determined (0.709, 0.708). For NBS 706, which has a smaller polydispersity (for the main body), the effect is smaller and the value -20 µl overcorrects the effect (0.715, 0.715). For BASF 168N, which has a broader distribution and a higher molecular weight, the effect is much stronger and the value -20 µl undercorrects the effect (0.682, 0.689). Finally, PS-IUPAC, which has a smaller molecular weight but a broader distribution, is

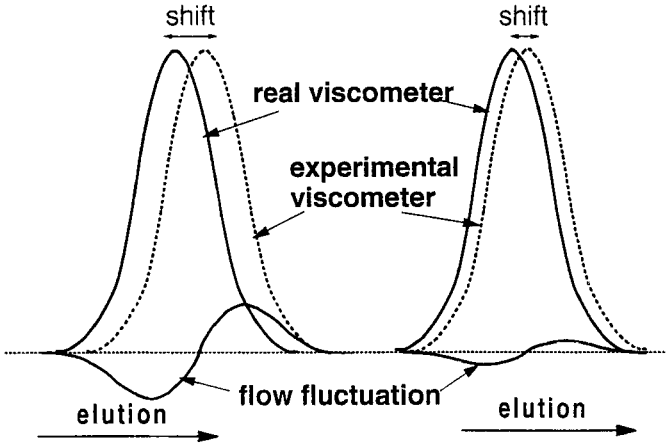

Figure 9. Influence of specific viscosity on apparent peak shift.

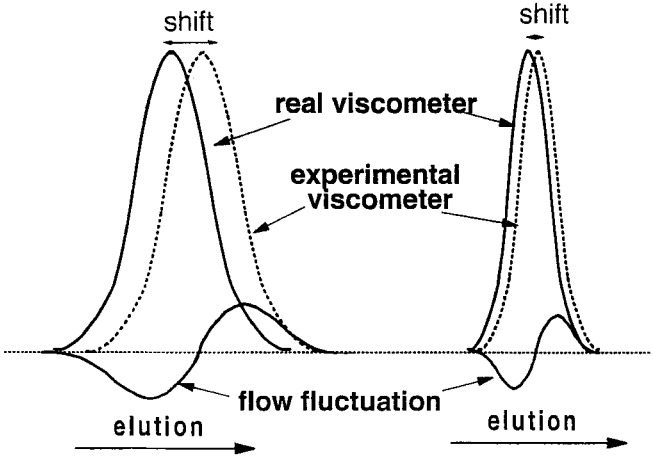

Figure 10. Influence of polydispersity on apparent peak shift.

calculated quite well (0.705), there is compensation between molecular weight and polydispersity for this sample.

The results of Table 4 ([η], a), in addition to the polydispersity "dis" and the concentration C, were entered into a regression software (Eureka from Borland) in order to determine if there was a relationship between those parameters. The following general relationship was obtained:

$$[\eta]^*C * dis^{0.5} * a^4 = 31.25$$

This relationship is valid only for polystyrene and under our experimental conditions. It means that the fluctuation depends directly upon the [η]*C value and upon the square root of the sample polydispersity.

Is it possible to correct this effect ?

This effect, depending simultaneously on three important parameters, the sample concentration C, the molecular weight (intrinsic viscosity [η]) and the polydispersity "dis", should have a different intensity for every sample. It appears quite impossible to set a perfect correction procedure with the software. Furthermore, we have just analyzed the situation in terms of peak shift when it is really a very small peak distortion.

What is the solution ?

The solution is obviously in the hardware. Every 0.009" capillary tube must be removed from the detector area and be replaced by tubes with larger internal diameter. This is true not only for the DRI inlet tubing, but also for every connecting tube between the columns and the several series-connected detectors. This is particularly valid when an external detector is used, such as a UV detector or a light scattering detector. The usual design uses long connecting capillaries to go into and out of the model 150CV, 0.009" tubes being used to minimize dead volumes. This can produce strong flow fluctuations. To avoid this, tubes with higher internal diameters must be used, but with a much shorter length in order to maintain minimal dead volumes. This requires more compact designs.

The internal geometry of the DRI detector must also be changed according to the same rules, i.e., higher internal diameter and shorter length. This has already been done and several DRI prototypes were tested successfully (9,10).

To check this proposed solution, the same simulation program was used, with different parameters, to study the behavior of DRI prototypes:

- the column set is still represented by a large number of 20 µl slices.

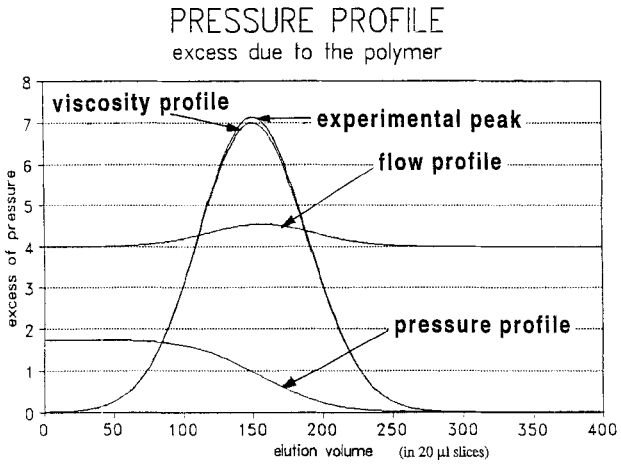

Figure 11. Computer simulation of the flow fluctuation and the viscometric signal distortion on an instrument equipped with a DRI prototype.

- the viscometer is still one slice of 0.014" tubing.
- the DRI inlet tubing is six slices (120 µl) of 0.020" tubing.
- the DRI outlet tube is still a great number of 0.040" slices.

The result of the simulation is represented in Figure 11; it should be compared to the one represented in Figure 5.

- the pressure profile is drastically changed. There is now a smooth decrease of pressure, corresponding to the polymer coming out the system. The pressure increase has completely disappeared.

- the flow profile is also completely changed. The flow fluctuation completely disappeared and there is now only a very small, quite negligible variation, corresponding to the polymer coming out the system. It is important to notice that the scale of the flow profile was amplified to show the fluctuation. The flow profile in Figure 11 must be compared to the one in Figure 5 where the fluctuation intensity is 0.04% of flow. They are plotted at the same scale factor.

- the experimental peak is now quite identical to the viscosity profile and there is no evidence of a peak shift; there is only a very small increase in intensity corresponding to the polymer coming out the system. This kind of profile is obviously within the standard error in detection and must certainly lead to a perfect determination of the viscosity law and the correct values of the Mark-Houwink K and **a**.

CONCLUSION.

The flow fluctuation, when the polymer peak comes across the detectors, is produced by the variation of pressure drop in the detectors, due to the specific viscosity of the polymer solution. It may occur in every system using capillary tubes (0.009") in the detector area. It is particularly visible on flow-sensitive detectors such as the SCV.

This effect is not reproducible from one instrument to another, since it depends on the internal diameter of the capillary tubes to the 4th power (Poiseuille's law), and capillaries are not reproducible. The example given in this paper is probably the worst case never encountered and the largest intensity never recorded. Many other 150CVs have been tested with a much smaller effect.

The intensity of the effect depends upon three main parameters (concentration, molecular weight and polydispersity of the sample); it is quite impossible to control it and to correct it with a software procedure. The only way is to change the hardware to reduce pressure drop in the detector area. Some DRI prototypes have been successfully built and tested with a geometry based on the rule: higher internal diameter and smaller length of connecting tubes. The results will be published in further papers (9-11).

The effect does not involve only the DRI detector but also any detector having a strong pressure drop or any arrangement between several detectors that involves long capillary tubes. Of course, the problem occurring with 0.009" tubings, any arrangement using smaller tubings like the 0.005" capillaries will produce much stronger effects.

A good practice for GPC using several detectors is to use more compact arrangements and connecting tubes with the highest possible internal diameters and the shortest possible length.

REFERENCES.

1. H. Benoit, P. Rempp and Z. Grubisic, J. Polym. Sci., B5, 753 (1967).
2. A.C. Ouano, J. Polym. Sci., Part A1, 10, 2169 (1972).
3. J. Lesec and C. Quivoron, Analusis, 4, 399 (1976).
4. D. Lecacheux, J. Lesec and R. Prechner, French Pt. 82402324.6 (1982), US Pt. 4478071 (1984), J. Appl. Polym. Sci., 27, 4867 (1982).
5. J. Lesec, D. Lecacheux and G. Marot, J. Liq. Chromatogr., 11, 2571 (1988).
6. C. Kuo, T. Provder, M.E. Koehler and A.F. Kah, ACS symposium series No 352, T. Provder Ed., 130 (1987).

7. J.L. Ekmanis, Waters Int'l GPC Symposium 89, Newton (1989).
8. J. Lesec, 1st Int'l Symposium on GPC/Viscometry, Houston (1991).
9. T. Huard, W.A. Dark, J.L. Ekmanis, T.J. Havard, R. Nielson and J. Lesec, 1st Int'l Symposium on GPC/Viscometry, Houston (1991) Waters Int'l GPC Symposium 91, San Francisco (1991).
J. Lesec, M. Millequant and T.J. Havard, Am. Chem. Soc., Polym. Mater. Sci. Eng., NEW-YORK, 65, 138 (1991); Gel Permeation Chromatography: Characterization by SEC and FFF, ACS series 521, T. Provder ed., 220 (1993).
10. J. Lesec, M. Millequant and T. Havard, Waters Int'l GPC Symposium 91, San Francisco (1991).
11. J. Lesec and T. Havard (to be published).

Received: October 12, 1993
Accepted: October 19, 1993